Dynamic Gust, Landing, and Taxi Loads Determination in the Design of the L-1011

Warren A. Stauffer* and Frederic M. Hoblit†
Lockheed-California Company, Burbank, Calif.

The approaches used to obtain dynamic gust, landing, and taxi loads in the design of the Lockheed L-1011 TriStar transport are described. The dynamic gust loads were determined in accordance with power-spectral concepts, utilizing a combination of mission analysis and design envelope criteria. Landing loads were based on conventional time history analyses. Taxi loads were obtained statistically from time history analyses in which taxi on surveyed runway profiles was simulated. A major part of both the gust and taxi load determinations consisted of generating matching conditions that enveloped the statistically defined loads.

Introduction

REFERENCE 1 provides an over-all view of the approaches used in establishing structural design loads for the Lockheed L-1011 TriStar, together with a description of the specific procedures used in the generation of the static aeroelastic load conditions. The purpose of this companion paper is to describe the approaches used to define the dynamic loads conditions—that is, those conditions for which inertia forces associated with accelerations in the elastic modes are significant and must be included. For the L-1011, these consisted of the gust, landing, and taxi conditions.

The L-1011 dynamic loads generation generally used the same basic grid systems, matrix algebra approach, and sources of basic data as the static aeroelastic analysis; these are described in Ref. 1.

Criteria for dynamic loads conditions are generally less well established than for static loads conditions. Development of suitable criteria, therefore, is a major consideration in dynamic loads work; the criteria used for the L-1011 are covered rather fully herein. Also treated in some detail is the matching condition technique, whereby design conditions for stress analysis and test are generated, which envelope the statistically defined gust and taxi loads.

Gust Criteria and Loads

Criteria and General Approach

In assuring adequacy of the L-1011 structure to withstand loads due to atmospheric gusts, primary reliance was placed on dynamic gust loads determined in accordance with power spectral, or continuous turbulence, concepts. Those loads provided the designing conditions for major portions of the wing, the vertical tail, and the fuselage in side bending, and for the engines and their supporting structure. Gust loads were also obtained on a static discrete gust basis, using the gust formula of FAR 25; the static gust loads, however, were generally not critical. In addition, as a requirement for British (ARB) certification, a tuned discrete gust analysis was performed to establish that loads thus defined would not exceed the airplane strength.

Received November 10, 1972; revision received March 9, 1973.
Index categories: Aircraft Structural Design (Including Loads); Aircraft Gust Loading and Wind Shear; Structural Dynamic Analysis.

*Chief Engineer—Structures. Member AIAA.
†Research and Development Engineer, Commercial Engineering Loads. Member AIAA.

The emphasis given to the power spectral gust loads resulted from a long-held conviction that the idealization of the gust environment as continuous turbulence is far more realistic than its idealization as a collection of individual gusts of simple geometrical shape and of intensity independent of gradient distance. Even traverses of thunderstorms usually result in gust velocity profiles having very much the appearance of continuous turbulence. Although individual gusts do sometimes occur, it is believed that the power spectral approach accounts much more realistically for the actual mix of gust shapes and gradient distances, and for the variation of gust intensity with gradient distance, than does any available discrete gust approach. As new airplanes are developed that differ from the older airplanes in their gust response characteristics, it is important that the most realistic available representation of the gust environment be utilized in their design. Only in this way can we be assured that the good service experience of the older airplanes will be repeated with the newer ones.

The L-1011 dynamic gust loads were obtained generally in accordance with criteria developed by the authors' company under contract with the FAA, in 1964–1966, and presented in report FAA-ADS-53 (Ref. 2). These criteria are considered by the FAA to be an acceptable means of compliance with the provision of FAR 25.305(d), that the dynamic response of the airplane to vertical and lateral continuous turbulence must be taken into account.

The power-spectral gust loads criteria developed in Ref. 2 are of two basic types—mission analysis and design envelope. As recommended therein, both of the two basic types of criterion were applied in determining the L-1011 dynamic gust loads. The primary effort involved the mission analysis criterion, as this generally gave the more severe loads. Sufficient design envelope work was then done to assure that the resulting loads would not be critical.

Mission Analysis Criterion

Under the mission analysis criterion, a set of typical flight profiles is first established. For the L-1011, these consisted of a long range profile, two intermediate range profiles, two short range profiles, and a pilot training and check flight profile. For the five operational profiles, payload was based upon a 70% passenger load factor and 5000 pounds of cargo. The two intermediate range flights, and likewise the two short range flights, differed only in the reserve fuel quantities. For one profile of each pair, the reserve fuel was a normal minimum, while for the other it was much larger, such as to permit additional flight without refueling. The fraction of flights in each of the six profiles was established according to careful esti-

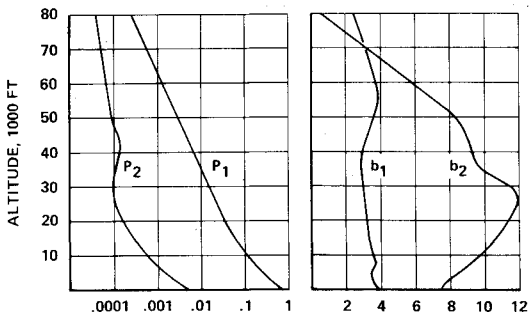

Fig. 1 Variation of gust probability parameters with altitude.

mates of the probable usage of the airplane. Two "mixes" were established, one favoring the high fuel weight profiles and one the low fuel weight profiles; design loads were based on the more severe of the two. The six profiles were then divided into a total of 59 segments for analysis. After combining similar segments from the various profiles, 35 distinct flight conditions remained for which dynamic analysis was performed.

The standard set of gust statistics established in Ref. 2 involves use of the Von Kármán shape of power spectral density with a scale of turbulence, L, of 2500 ft. The probability distribution of the rms gust velocity is defined in a form such that the frequency of exceedance of each load quantity in any given flight segment is given by the expression

$$N(y) = N_0\left[P_1 \exp\left(-\frac{y/\bar{A}}{b_1}\right) + P_2 \exp\left(-\frac{y/\bar{A}}{b_2}\right)\right]$$

In this expression, y can be any load quantity—for example, bending moment at a particular wing station. $N(y)$ is the number of exceedances of y per unit time. $\bar{A}$ is the ratio of the rms value of y to the rms gust velocity, and N_0 is a characteristic frequency of y, obtained as the radius of gyration of the power spectral density of y about zero frequency. Both $\bar{A}$ and N_0 are obtained by appropriate dynamic analysis, as described below. The constants P_1, P_2, b_1 and b_2 are parameters defining the gust environment; plots are provided in Ref. 2 as a function of altitude (Fig. 1). These values of the P's and b's were adapted from those presented in Ref. 3. Exceedances are calculated by the above equation for each mission segment and then added to give a total for the over-all operation of the airplane. Subtotals are also obtained for each profile. For the vertical gust analysis, the above equation for $N(y)$ is modified to include the contribution of the one-g steady flight loads, so that the exceedances obtained are of net loads.

For the L-1011, vertical gust exceedance curves were computed and machine plotted for each of 95 load quantities. An example of the curves thus obtained is shown in Fig. 2. In the vertical gust analysis, because of the presence of the one-g load, separate curves were needed for positive and negative loads. Each of these exceedance curves was then entered with the limit design frequency of exceedance of 2×10^{-5} cycles/hr (once in 50,000 hr) to give the limit design value of the load.

The limit design value of frequency of exceedance was established in Ref. 2 as the frequency of exceedance of limit strength of past satisfactory airplanes, determined by dynamic analysis of three specific airplanes utilizing the particular gust environment defined therein. Because of the satisfactory safety record of these airplanes, this design level is considered adequate. It may conceivably be higher than necessary; yet calculated probabilities of exceedance of the limit or ultimate strength of these airplanes generally indicate that no significantly lower level of strength would be desirable. By fortunate coincidence, the frequency of exceedance of limit strength was approximately the same for all three of the airplanes studied, the Lockheed Constellation and Electra and the Boeing 720B.

The mission analysis approach provided a convenient means of accounting realistically for the load reduction due to the presence of a yaw damper. In the L-1011 lateral gust analysis, exceedance curves were obtained separately with and without the yaw damper included. These curves were then combined on the assumption that the yaw damper would be inoperative 3% of the time and operative the remaining 97% of the time. The estimate of 3% of the time is believed to be extremely conservative, inasmuch as the yaw damper is a two channel system, is fully effective with only one channel operative, has an expected failure rate per channel of less than 0.001/hr, and is required to have one channel operative for dispatch. The net reduction in lateral gust design loads achieved through use of the yaw damper was 20%. With no account taken of time inoperative, the reduction would have been 28%. The loads with yaw damper operative included a 5% increase to account for the slight degradation in yaw damper effectiveness at the limit load level due to saturation. This is a nonlinear effect and cannot, of course, be accounted for directly in the power spectral analysis. The percentage used was determined from analog computer simulations in which an appropriate continuous turbulence gust time history was used as an input, at several intensities, and the airplane representation included the limiting rudder hinge moment.

Design Envelope Criterion

Under the design envelope criterion, all considerations of actual operational usage are ignored. Instead, design is to the specified design envelope of speed, altitude, gross weight, fuel weight, zero-fuel weight, and c.g. position. In this respect, the criterion is similar to the past discrete gust criteria, as well as to prevailing limit design maneuver loads criteria. Under this form of criterion, a shape of gust power spectral density function is again selected; this is taken, as in the mission analysis criterion, as the Von Kármán shape with $L = 2500$ ft. A quantity $\sigma_w \eta_d$, which is analogous to a design gust velocity, is then specified as a function of altitude, on the basis of a roughly constant

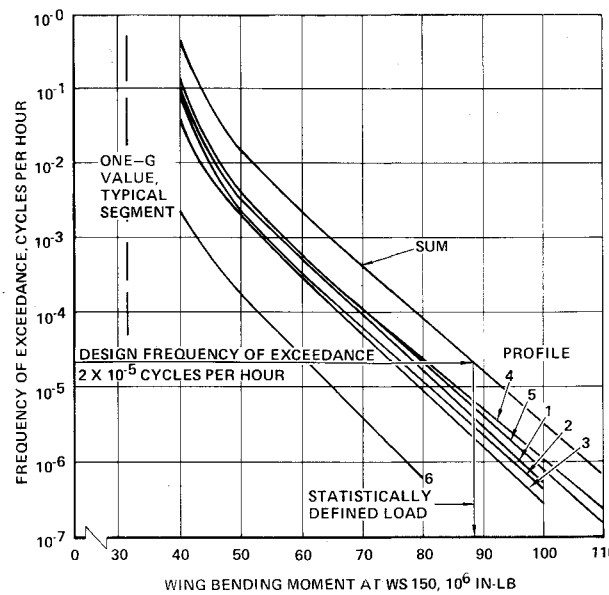

Fig. 2 Typical frequency-of-exceedance curves.

frequency of exceedance. In the expression $\sigma_w\eta_d$, σ_w is a design rms gust intensity and η_d is a factor representing the ratio of design load to rms load. The breakdown between the two factors is ordinarily not of consequence except as an aid in visualizing the physical significance of the parameter. The design load at any point is then given by multiplying $\sigma_w\eta_d$ by $\bar{A}$:

$$y_d = \sigma_y\eta_d = (\bar{A}\,\sigma_w)\eta_d = \bar{A}(\sigma_w\eta_d)$$

Under this form of criterion, as under the mission analysis criterion, the design level is set to match the limit strength of past satisfactory airplanes. Amongst the three reference airplanes analyzed in Ref. 2, limit strength values of $\sigma_w\eta_d$ varied from about 60–110. To assure adequate strength in the absence of a mission analysis, it would appear that a value well above the bottom of this range would be required. On the other hand, the lowest value, 60, represents the limit strength of an airplane with satisfactory service experience. This level is recommended in Ref. 2 for use in conjunction with a mission analysis as a floor below which the design gust loads should not drop. Such a floor provides insurance against omitting pertinent operational elements in setting up the mission profiles and breaking them into segments. It also provides insurance against a possible rapid increase in gust response as the boundaries of the design envelope are approached.

The actual value of $\sigma_w\eta_d$ as a function of altitude, recommended in Ref. 2 for use as a design envelope floor, varies linearly from 56 fps at sea level to 62 fps at 7000 ft to 55 fps at 27,000 ft to 17 fps at 80,000 ft. These values apply at speed V_C. Reflecting the philosophy of the older discrete gust criteria, values of 1.32 times those quoted apply at speed V_B and 0.50 times those quoted apply at speed V_D.

L-1011 design envelope loads were obtained using these $\sigma_w\eta_d$ values. These loads exceeded the mission analysis loads locally at some points in the structure; but at these points it so happened that loads given by other types of condition were critical. Thus at no point in the airplane did the design envelope loads design the structure.

Dynamic Analysis

Separate vertical gust and lateral gust dynamic analyses were employed to obtain $\bar{A}$ and N_0 values of the various airplane loads. In these analyses, the equations of motion used as generalized coordinates 20 elastic modes (natural vibration modes of the free airplane) and either two or three rigid-body modes—plunge and pitch in the vertical gust analysis, and sideslip, yaw, and roll in the lateral gust analysis. These equations were solved to give frequency-response functions at 100 to 140 different frequencies, ranging from 0.00005 cps to about 14 cps. The frequency-response functions were obtained for 95 load quantities in the vertical gust analysis and 93 in the lateral gust analysis. Multiplication of the gust input power spectral density by the square of the modulus of the frequency-response function gave the response power spectral density. This was then integrated to give $\bar{A}$ and N_0 values.

Mass, stiffness, and aerodynamic data were provided in the form of panel weights, structural (deflection) influence coefficients, and aerodynamic influence coefficients on appropriate grids as described in Ref. 1. In the dynamic gust analysis, forces were lumped on a coarser grid consisting of 99 points for the vertical gust analysis and 125 points for the lateral gust analysis.

Unsteady aerodynamic effects were approximated by considering lift growth at all points on the airplane to occur in accordance with a single indicial function, $1 - a \exp(-bt)$, where a and b are functions of aspect ratio and Mach number such as to best approximate the lift growth on a rigid wing. The gradual penetration of the airplane into the gust was accounted for in accordance with the geometry of the 99 or 125 lump points. For a limited number of cases, the vertical gust analysis was also run using complex aerodynamic influence coefficient matrices obtained from kernel function solutions for oscillatory motion.[1,4] The most important effect of the oscillatory aerodynamics was found to be to increase the aerodynamic damping in the first wing elastic mode. This increase amounted to 5% of critical (dead-beat) damping. Accordingly, in all the steady-aerodynamics solutions an additional external damping of this amount was introduced into this mode. It has now become feasible to use the oscillatory, or unsteady, aerodynamic influence coefficients in all routine vertical gust loads analysis, and this approach is planned for derivative versions of the L-1011.

Matching Condition Generation

A major obstacle to the acceptance of power-spectral methods for design gust loads determination, that has long been recognized, is the difficulty in providing the loads information in a form suitable for stress analysis. Normal stress analysis practice utilizes design conditions each of which is defined over the whole of some major structural component at a given instant. Each such condition consists of a set of forces in equilibrium. Under such a set of forces, the stresses in each minute element of the structure can be determined; and the same set of forces can be applied in a static test. Power spectral methods, however, do not result in this sort of design condition. They lead, instead, to individual design-level values of load such as shear, bending moment, and torsion, at various points in the structure. These are defined statistically and generally do not occur simultaneously. Stresses within the structure are not defined until appropriate combinations of these loads—for example, wing shear and torsion at a given wing station—are defined, with regard to both sign and magnitude.

Various approaches have been proposed to avoid having to define dynamic gust design conditions. One is to determine design-level values of internal loads or stresses. This, manifestly, involves determining separate power spectra for loads in every element of the structure. Further, where the strength of an element such as a wing surface panel involves the interaction of two stresses, such as compression and shear, the actual interaction curve or strength envelope must be introduced into the power spectral analysis. Instead of determining a frequency of exceedance curve, for example, the frequency of exceedance of limit strength, as defined by the interaction curve, is found.

At the authors' company, it has been considered imperative actually to generate "design conditions" that "match" in realistic combinations the statistically defined loads resulting from the power spectral analysis. The concept of a design condition has long permeated the entire art of structural analysis. Inasmuch as the various design loading conditions are relatively uninfluenced by changes in the structure (short of major changes in the over-all stiffness), it has been possible to keep the loads determination function entirely distinct from the stress analysis and structural design functions. Design and optimization of the structure are thus facilitated. The usual refinements in the stress analysis methods as the design progresses are easily accommodated. Refinements in the loads determination can proceed independently of those in the stress analysis.

Procedures for generating these matching conditions are discussed and illustrated in Ref. 2. These procedures have been further developed as experience has been gained in

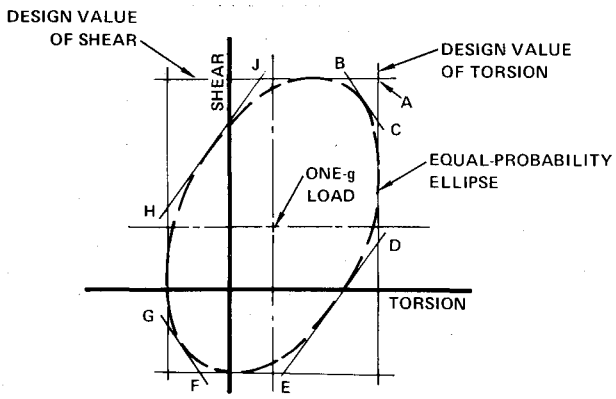

Fig. 3 Equal-probability shear-torsion ellipse and circumscribing octagon.

their use, and they were applied successfully on the L-1011. They were used, moreover, in matching not only the power spectral gust loads, but also the taxi loads defined statistically by means of time history simulation of taxiing on surveyed runway profiles. Later in the L-1011 development program, the matching condition approach was also used to define buffet loads for stress analysis in the aft-body and empennage region, consistent with empennage loads and aft-engine accelerations measured during FAA demonstration stalls.

Basic Concept

The basic concept employed in matching-condition generation is suggested by the fact that, in flying through turbulent air, an airplane responds statically to the low frequency components of the turbulence (long gradient gusts) and it responds dynamically in its various elastic modes to the higher frequency components of the turbulence. The two types of response—the static and the dynamic—generally have quite different distributions of load throughout the structure. Moreover, each elastic mode will have its own distinctive load distribution. In flight through typical turbulence there is a random interplay amongst these various distributions. As a result, no single distribution that might be applied can be expected to reproduce simultaneously the correct stress histories at all points in the structure.

Accordingly, in generating matching conditions, the approach is to start with a number of elementary distributions. Each of these consists of a set of forces in equilibrium, representing the static response of the airplane or the dynamic response in a particular elastic mode. These elementary distributions, as building blocks, are then superimposed in various proportions to give a number of design conditions which, collectively, envelope the statistically defined shears, bending moments, and torsions. Further, this enveloping takes proper account of the phasing of the various load quantities, such as shear and torsion at a given wing station. It thus provides, for example, the proper amount of torsion in combination with the maximum shear and the proper shear with the maximum torsion. The procedure is essentially one of trial and error; the work can be systematized, however, in such a way as to permit homing in fairly rapidly on each desired condition.

Preparatory Steps

In describing in more detail the matching condition generation as carried out on the L-1011, the matching of wing loads due to vertical gust will be used as an example. Fuselage loads due to vertical gust were matched similarly.

The first step in generating the L-1011 matching conditions was to list the design-level values read from the frequency-of-exceedance curves. For the wing, these consisted of shears, bending moments, and torsions at nine wing stations. These were designated, collectively, L_E (L for load, E for exceedance).

The second step was to select a particular flight segment typical of those that predominated in determining the exceedance curves. The segment selected was the cruise segment of the short-range high-reserve-fuel profile.

The one-g loads for this typical profile were then subtracted from the L_E loads to give loads designated L_S. These became the statistically defined loads to be matched. Net design loads would later be obtained by adding loads for this same one-g condition to the various conditions matching the L_S loads.

Next, the elementary distributions were obtained. Each of these consisted of a set of panel loads in equilibrium, defined over the entire airplane. Shears, bending moments, and torsions were obtained for each elementary distribution and listed; these were designated, collectively, E_1, E_2, . . . The symbol E_1, for example, designated the loads of the first elementary distribution, E_2 the second, etc. The elementary distributions consisted of the following: 1) static aeroelastic loads due to a one-g static discrete gust; these in effect are loads due to an arbitrary angle of attack, with the air loads reacted by plunge and pitch inertia; 2) static aeroelastic loads due to a unit pitch rate; and 3) for each of seven selected natural vibration modes, the inertia forces associated with unit $\ddot{q}$ (generalized acceleration) together with airloads occurring at the associated modal displacement, q. To determine the value of q associated with unit $\ddot{q}$ in each mode, it was noted that the static response in each mode is already accounted for in the static distributions. The desired value of q, therefore, is that associated with dynamic overtravel in the mode. By equating the generalized inertia and aerodynamic forces in the mode and ignoring the gust forces as negligible at the resonant peak, it can be shown that $q = -\ddot{q}/\omega_n^2$, where ω_n is the natural radian frequency of the mode. Inasmuch as the predominant contribution of each mode to airplane response occurs at the resonant frequency, the aerodynamic forces associated with q, calculated on a zero-frequency basis, were multiplied by the real part of the lift-growth function at the resonant frequency. Also, since the aerodynamic forces associated with q were generally not in equilibrium, they were balanced with the necessary rigid-airplane pitch and plunge inertia. (The forces associated with $\ddot{q}$ were already in equilibrium because of the inherent properties of a vibration mode. The static aeroelastic distributions, Items 1 and 2 in the foregoing, were also in equilibrium, as they were obtained by the same methods as the static design loads.[1])

All of these elementary distributions were calculated using data for the predominant mission segment, selected as noted in the foregoing.

The elementary distributions are seen to reflect very closely the actual distributions which superimpose in various proportions, instant by instant, in actual flight through turbulence. In combining these elementary distributions to form design conditions, no more of each should be used than would occur at the same frequency of exceedance as the loads being matched. Accordingly, an approximate design-level value of the coefficient, or generalized coordinate, associated with each of the elementary distributions was calculated. These values were given by $\bar{A}$ $(\sigma_w \eta_d)$. In this expression, $\bar{A}$ is the value appropriate to each of the generalized coordinates—Δn_{cg}, $\ddot{\theta}$, $\ddot{q}_1$, $\ddot{q}_2$, etc.; it is obtained from the dynamic analysis for the predominant segment selected above. The quantity $\sigma_w \eta_d$ is

Table 1 Matching condition generation—sample table of $\bar{E}$ values

Load quantity Type	Locations Wing Sta.	$\bar{E}_1$ Δn	$\bar{E}_2$ $\dot{\theta}$	$\bar{E}_3$ Mode 1	$\bar{E}_4$ Mode 2	$\bar{E}_5$ Mode 3	$\bar{E}_6$ Mode 4	$\bar{E}_7$ Mode 5	$\bar{E}_8$ Mode 6	$\bar{E}_9$ Mode 7
	217	0.65	0.01	0.29	0.11	0.10	−0.09	−0.17	0.01	−0.10
Shear	419	0.71	0.04	0.34	0.02	0.02	0.00	−0.12	−0.01	−0.03
	684	0.37	0.02	0.84	−0.01	0.00	0.13	0.03	−0.02	−0.05
	217	0.65	0.03	0.50	0.06	0.02	0.02	−0.10	−0.01	−0.03
Bending	419	0.58	0.04	0.60	0.01	0.01	0.09	−0.03	−0.02	−0.05
moment	684	0.48	0.04	0.68	0.00	0.00	0.20	0.18	−0.01	−0.06
	217	0.51	−0.01	−0.07	0.47	0.24	0.48	−0.06	−0.06	0.26
Torsion	419	0.60	0.03	−0.43	0.03	0.02	0.01	0.01	−0.07	−0.21
	684	0.32	0.04	−0.80	0.03	0.01	−0.07	−0.05	−0.07	−0.27

the value (actually an average value) by which the wing load $\bar{A}$'s for the same segment would have to be multiplied to give their respective L_S values. In order to facilitate the actual matching operation discussed below, it is desirable to modify each elementary distribution by multiplying throughout by the coefficient thus determined. The elementary distributions thus are normalized to their design-level values.

As a final preparatory step before starting the actual condition matching, correlation coefficients between shear and torsion, and between bending and torsion, were obtained at each of nine wing stations. The predominent mission segment previously selected was used for this purpose. The correlation coefficient, ρ, is obtained readily from the frequency-response functions, utilizing an expression derived from Appendix B of Ref. 5,

$$\rho = \frac{1}{\bar{A}_x \bar{A}_y} \int_0^\infty \phi_w [(H_x)_{\text{real}}(\omega)(H_y)_{\text{real}}(\omega) + (H_x)_{\text{imag.}})(\omega)(H_y)_{\text{imag.}}(\omega)] d\omega$$

where x and y are the two load quantities, ϕ_w is the gust power spectral density, and H is the frequency-response function in complex form.

The correlation coefficient, ρ, is the key to establishing realistic combinations of shear and torsion, and of bending and torsion, at each wing station. The correlation coefficient establishes an equal-probability ellipse, such as shown by the dash line in Fig. 3. Ideally, an infinite number of design conditions might be defined, matching every point around the ellipse. In practice, an attempt is made to match approximately the eight corners of the circumscribing octagon, BCDEFGHJ. For the L-1011, the circumscribing octagons were constructed for shear-torsion and bending-torsion interaction at all nine wing stations at which ρ's were obtained. The construction was accomplished by means of curves such as shown in Fig. 4.

Table 2 Matching condition generation—sample table of L_D/L_S values

Load Quantity		L_D/L_S Values					
Type	W. Sta.	Cond. 1	Cond. 2	Cond. 3	Cond. 4		Cond. 14
	217	.96	1.02	.89	.59		.68
Shear	419	.86	1.02	.87	.68		.92
	684	.99	.86	.34	.36		.94
	217	.97	1.03	.81	.65		.91
Bending	419	.94	.99	.63	.56		.99
Moment	684	.82	.80	.33	.54		1.04
	217	.07	.85	1.02	1.03		.32
Torsion	419	.06	.70	.59	.49		.29
	684	-.35	.28	.36	.15		-.25
Coefficient		Values of Coefficients Defining Each Condition					
a_1		.60	1.07	1.00	1.00		1.00
a_2		0	-1.00	.67	.67		1.00
a_3		.97	.43	0	0		.58
a_4		.55	.25	.85	.75		-.75
a_5		0	0	0	0		0
a_6		-.34	.69	0	0		.57
a_7		-.52	-.96	-.96	.42		.10
a_8		.97	-1.02	0	0		.97
a_9		-.88	-.96	.21	.74		0

Matching

The various design conditions were then generated. Each condition consisted of a certain amount a_1 of the E_1 distribution, a certain amount a_2 of the E_2 distribution, etc. Assignment of a set of values to the coefficients a_1, a_2, ... a_9 thus defined a complete set of panel loads, as well as a set of shears, bending moments, and torsions. Letting L_D designate collectively the shears, bending moments, and torsions in one design condition,

$$L_D = a_1E_1 + a_2E_2 + \ldots + a_9E_9$$

A new set of values of the coefficients a_1, a_2, ... a_9 would then define a second design condition, and so on.

For the L-1011 wing, a total of about 30 design conditions was found to be necessary to envelope adequately the loads on the entire wing. At a given wing station, about 12 conditions were necessary to envelope both the shear-torsion and bending-torsion equal probability ellipses (Fig. 3). The same conditions might match fairly well at several adjacent wing stations, but to cover the entire span additional conditions were needed.

The actual generation of matching conditions was systematized by the use of two types of table, shown as Tables 1 and 2. The tables as shown have been abbreviat-

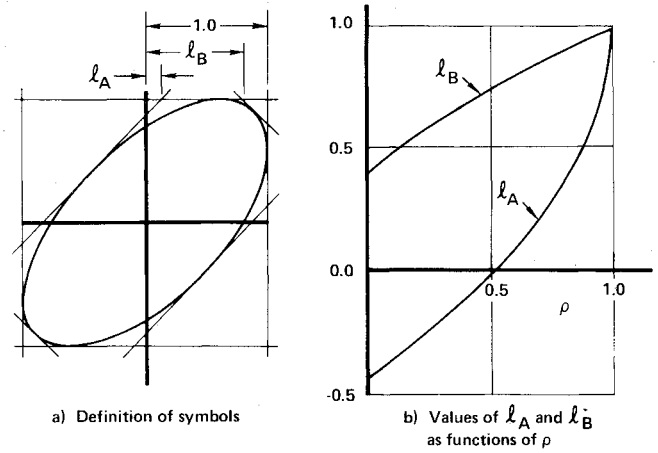

Fig. 4 Geometric properties used in constructing equal-probability ellipses.

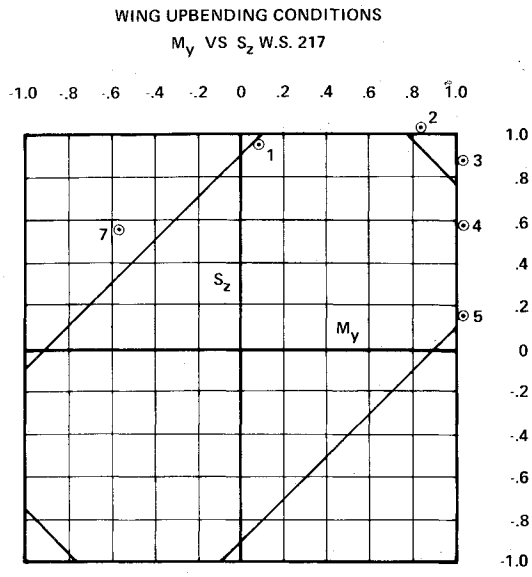

Fig. 5 Matching condition generation—sample shear-torsion diagram.

ed for illustrative purposes; the original tables included loads at nine rather than three wing stations, engine y and z load factors, and two fuselage loads; and the values were given to one more significant figure. Also, the numbers in the tables have been modified to reflect normalization of the elementary distributions to design-level values. This normalization has been standard practice for some time in Lockheed taxi loads work but has only recently been introduced into the gust condition-matching.

Table 1 lists values of $\bar{E}$ defined as E/L_s. The usefulness of this table derives from the expression for L_D/L_S. Noting that, for any condition,

$$L_D = a_1E_1 + a_2E_2 + \ldots + a_9E_9$$

it follows that

$$\frac{L_D}{L_S} = a_1\frac{E_1}{L_S} + a_2\frac{E_2}{L_S} + \ldots + a_9\frac{E_9}{L_S}$$

$$= a_1\bar{E}_1 + a_2\bar{E}_2 + \ldots + a_9\bar{E}_9$$

Once a given condition has been satisfactorily generated, L_D/L_S will be approximately unity for one or hopefully several of the load quantities and less than unity for all others. Scanning the table of $\bar{E}$ values (Table 1) one can quickly obtain first-estimate values of the a's. For example, from the $\bar{E}_1$ column, it is clear than an α_1 value of 1/0,71 = 1.41, with all other a's = 0, will match wing shear (i.e., make $L_D/L_S = 1$) in the region of WS 419 and leave L_D less than L_S (i.e., $L_D/L_S < 1$) for all other load quantities. But for a realistic match the amount of E_1 should not substantially exceed its design-level value—that is, a_1 should not substantially exceed unity. Hence a_1 will be reduced and the difference made up from other distributions, chiefly E_3. (It is seen that if one takes $a_1 = a_3 = 1.00$, L_D/L_S for shear at WS 419 will be 0.71 + 0.34 = 1.05, or more than required.) Inasmuch as the $\bar{E}_3$ values are greater for other load quantities than for shear at WS 419, it might be expected that introducing a substantial amount of this distribution would actually provide a closer match over more of the wing than use of the E_1 distribution alone.

Table 2 shows the L_D/L_S values for each of the final matching conditions. A similar table is filled out as successive trials are made in iterating toward each condition. Condition 2 is the condition that was initially intended to match shear at WS 419. The value of a_1 is seen to have been reduced from 1.41 to 1.07. The various amounts of the other distributions serve not only to offset the reduction in a_1, but also to increase the spanwise extent of the match and to tailor the torsions to the values indicated as appropriate by the equal-probability ellipses. For the latter purpose, 18 nondimensional shear-torsion and bending torsion plots were provided as illustrated in Fig. 5. As iteration proceeds, the results are spotted on these plots as well as entered into Table 2. Table 1 used in conjunction with Table 2 continues to provide a guide as to which distributions to bring in and in what magnitude as the matching proceeds.

The arithmetical work involved was facilitated by use of a remote access computing system. The various E and L_S values were stored in the computer; and as each new trial set of a's was submitted, a complete set of L_D/L_S values was immediately typed out. Currently, techniques based on optimization theory are under development which, it is hoped, will permit much of the actual matching operation to be carried out automatically by computer on a batch processing basis.

Evaluation

It is believed that the stresses actually occurring throughout the wing during flight through turbulence will be reproduced realistically by the matching conditions if all of the following are satisfied:

1) The shear-torsion and bending-torsion ellipses are adequately enveloped at the nine wing stations at which defined. (The shear-bending phasing is less critical and is expected to more or less take care of itself.)

2) Each condition remains on or close to the equal-probability ellipse over a distance of several wing cuts.

3) The elementary distributions are reasonably representative of actual distributions associated with motions in the various static and elastic modes.

4) The coefficients do not exceed their individual design-level values; and where L_D/L_S = unity, the contributions of all the E's tend to be of the same sign.

If care is taken to satisfy Items 3 and 4, it is believed likely that item 2 will be satisfied as well.

As evident from simple beam theory, the stresses within a wing at any wing station are governed primarily by the shear, bending moment, and torsion at that wing station. Consequently, if the shear, bending, and torsion are correctly phased, the phasing spanwise is of minor importance.

Landing Gear Characteristics

The L-1011 landing gear system is conventional. It consists of two main landing gears, each with a four-wheel bogie, and a two-wheel steerable nose landing gear. The struts of all gears are of the air-oil type. The stroke of the L-1011 main landing gear is 26 in. This is somewhat greater than other large transport airplanes and results in correspondingly lower loads and accelerations in both landing and taxi. The nose gear stroke is 18 in.

The landing gear characteristics that most influence not only airplane loads, but also landing and taxi comfort and handling, are, in addition to the strut stroke, the air compression characteristics and the hydraulic damping characteristics.

In the conventional single-air-chamber strut, the fully-compressed and fully-extended air loads define the entire airspring curve. The fully-compressed load of the L-1011 gears was selected to provide a modest margin against bottoming of the strut at the limit design taxi load. An

excessive fully-compressed load would reduce the stroke available for absorbing landing impact and, by stiffening the air spring at static extension, result in higher taxi loads and accelerations. Selection of the fully-extended load requires a compromise, in the case of the main gear, between landing and taxi softness. To achieve a low spring rate at static extension, and thus a soft taxi ride, a high fully-extended load is desirable. On the other hand, to achieve soft landing under day-in-day-out low-sinking-speed conditions, the fully extended load must be low enough to permit stroking of the gear at a low load level. For the L-1011 main gear, the fully extended load is 0.20 times one-half the design landing weight. From the landing comfort standpoint, this value is considered adequate, on the basis of a careful comparison with other airplanes including consideration of the effect of bearing friction on the strut breakaway load. It also provides an excellent taxi characteristic. For the nose gear, landing comfort is a secondary consideration; but the fully-extended load should not be so high that the strut extends fully during normal taxiing at light weights. The L-1011 nose gear fully-extended load is equal to 64% of the static load at operating empty weight and aft c.g. limit.

For both main and nose gears, the metering system was such that, for the limit design landing condition, the hydraulic peak was substantially lower than the air peak. This characteristic results in lower spin-up and spring-back loads, lower fuselage dynamic loads, and a significantly more comfortable landing at intermediate to high sinking speeds. For the main gear, nearly optimum characteristics were obtained with a plain orifice; for the nose gear, a metering pin is used.

Landing Criteria and Loads

L-1011 landing loads were obtained generally in accordance with the criteria of FAR 25.

Landing gear loads were determined from time history analyses of each gear individually. The gear representation included the nonlinear tire load-deflection characteristic, the unsprung mass, isothermal air compression in the strut, hydraulic damping, strut O-ring (constant) and bearing friction, and strut fore-aft stiffness varying with strut closure. The airplane was considered rigid. Tire-to-ground friction was considered to vary with instantaneous skidding velocity in accordance with NASA data presented in Refs. 6 and 7. To investigate local loads in the bogie due to earlier contact of the rear wheels in a tail-down landing, the bogie pitch characteristics were also included.

Wing and fuselage dynamic landing loads were obtained on the basis of full dynamic accountability, for 10 fps symmetric landings. Fifteen symmetric elastic modes were used as generalized coordinates. Gear load inputs reflected the small alleviating effect of the airplane flexibility. Time histories of shears, bending moments, and torsions were obtained at various points in the wing and fuselage. At instants when load peaks occurred, generalized accelerations in all modes were read and panel loads computed therefrom. These were superimposed on the steady one-g approach flight loads to give net loads. These loads were the designing down-bending conditions for much of the fuselage.

Taxi Criteria and Loads

General Approach

In the absence of definitive FAR requirements for taxi loads, Lockheed has for many years been concerned with the establishment of realistic taxi loads criteria and methods. "Taxi loads" in this context refers to the loads produced by runway and taxiway bumps encountered during the takeoff run, landing runout, and taxiway taxiing.

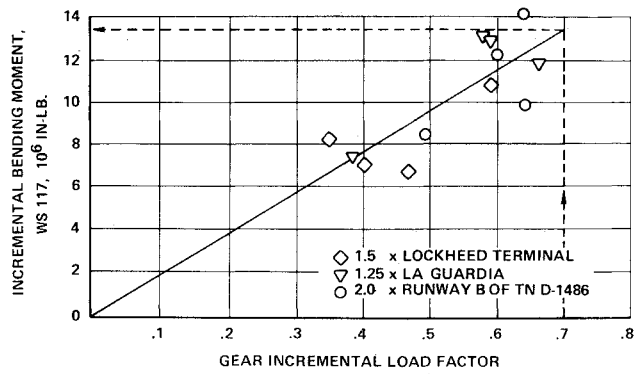

Fig. 6 Typical curve of analog taxi results.

All of the L-1011 taxi loads work has been based on a recognition that runway and taxiway bumps generally do not occur as isolated bumps of simple shape. Instead, they are of a variety of shapes and tend to occur as more or less continuous roughness. Accordingly, the L-1011 taxi loads determination has been based entirely on time history analyses in which taxi on actual runway profiles is simulated.

In these analyses separate profiles for left and right main gears are used, because of previous experience indicating that the antisymmetric as well as symmetric components of excitation and response are important. A separate profile for the nose gear track was generally not available; hence the nose gear profile was taken as identical to either the left or right main gear profile. (Obtaining a nose gear profile by averaging the left and right main gear profiles is not desirable, because the averaging results in a profile of reduced severity.) Eleven elastic modes—six symmetric and five antisymmetric—were included in the airplane representation, as well as the three rigid-airplane modes of plunge, pitch and roll. The elastic modes were free-airplane modes, obtained with mass and stiffness lumped on a 119-point (per half airplane) grid. The landing gear representations included a linearized tire spring, the unsprung mass, an isothermal airspring, hydraulic (square law) damping, and friction. In the design stage, the four-wheel bogie was not simulated. In later analyses, the effect of the four-wheel bogie in smoothing the bumps was approximated by modifying the profile, on the basis that the profile height felt by the gear at any instant would be the average of the heights at the forward and aft pairs of wheels. These later analyses indicated about a 10% reduction in load due to the averaging effect of the bogie. Both analog and digital procedures were available for carrying out these analysis. Most of the L-1011 work was done, however, using basically analog equipment.

The basic objective in establishing design taxi loads for the L-1011 was to provide consistent strength throughout the airplane structure, at a level such that limit strength will not be exceeded during the takeoff run on the roughest runways from which the airplane will be operated. Only the takeoff run is considered, because of NASA VGH data indicating that load factors occurring during taxiway taxiing are much lower than during the takeoff run or landing runout, and because of the lower airplane weights on landing runout than on the takeoff run.

To achieve this objective, the first step was to establish a design value of the main gear incremental load factor, defined as incremental load on one main gear divided by one-half the airplane gross weight. The second step was to establish loads throughout the airplane consistent with this value of the gear incremental load factor.

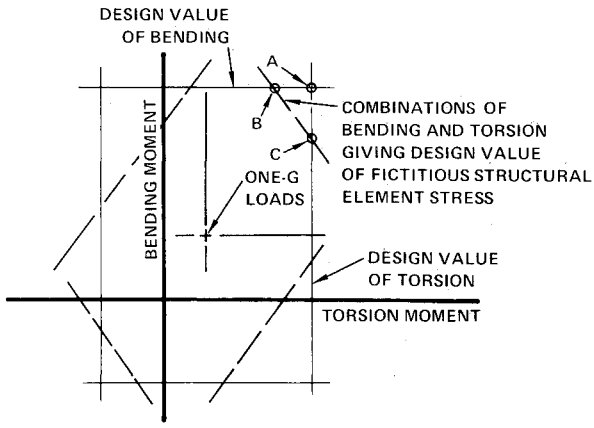

Fig. 7 Determination of design combinations of taxi-load bending and torsion moments.

Design Gear Incremental Load Factor

For the purpose of establishing the design incremental load factor, time history runs were made using the profiles of a runway which, on the basis of available surveyed profiles of many runways, appears to be as rough as any in general use by large transport airplanes.

Computer time history runs were made on this set of profiles at a number of constant speeds and with speed increasing during the run (from 30 to 120 knots) to simulate a takeoff run. Runs were made both with and without aerodynamic lift included. Aerodynamic lift has the effect of lightening the load on the gears, resulting in a softer oleo airspring and consequently lower incremental loads. With lift included, the conditions of a takeoff run were simulated; runs made without lift simulated a rejected takeoff, in which use of spoilers would leave virtually no lift. Representative results, obtained at a fairly early stage of design, are shown in Table 3. Based on these numbers, a design value of Δn_G of 0.70 was selected. For the takeoff run case (the with-lift column in the table) this value provides some margin for the possibility that there may be runways rougher than the one selected and from which the L-1011 will occasionally operate. It also provides for the slight increase in load factor that may occur at speeds above those for which runs were made. For the rejected takeoff case (no-lift) the margin is less, but still adequate in view of the very low frequency with which a rejected takeoff will occur at maximum weight on the roughest runways.

Statistically Defined Loads

With the design gear incremental load factor established, the second step was to determine loads throughout the airplane consistent with this incremental load factor. For this purpose, constant speed runs were made at 30, 60, 90, and 120 knots on each of three runways. Because of the landing gear nonlinearities, it was desired that the loads obtained include peaks at approximately the limit load level. Consequently, factors were applied to the profile heights to give adjusted profiles for use in the analyses. The profiles and factors were as follows: for La Guardia Runway No. 4 (survey of Oct. 1955), a factor of 1.25; for Hollywood-Burbank Airport E-W Runway (Aug. 1961), a factor of 1.50; for Runway B of NASA TN D-1486 (Ref. 8), a factor of 2.00. All of these runs were made with zero aerodynamic lift. Time histories were obtained of the vertical loads on all three landing gears, of the generalized accelerations in all rigid body and elastic modes, and of some 80 additional airplane loads and accelerations. The airplane loads included wing shears, bending moments, and torsions at several locations and fuselage shears and bending moments at several locations. These were obtained in the computer by superposing several sets of forces in equilibrium, namely: 1) symmetric component of main gear load reacted by rigid airplane pitch and plunge inertia; 2) antisymmetric component of main gear load reacted by rigid airplane roll inertia; 3) nose gear load reacted by rigid airplane pitch and plunge inertia; and 4) elastic mode inertia force distribution for each elastic mode. Each internal load time history was thus calculated by means of an expression,

$$\text{Load} = C_1P_{\text{sym}} + C_2P_{\text{anti}} + C_3P_{\text{nose}} + C_4\ddot{q}_1 + C_5\ddot{q}_2 + \ldots + C_n\ddot{q}_{n-3}$$

where the C's are constants appropriate to the particular load being obtained, the P's are the gear load time histories, and the $\ddot{q}$'s are the elastic mode generalized acceleration time histories.

To obtain loads throughout the structure consistent with the gear incremental load factor of 0.7, the results of the 12 time history runs were plotted as shown in Fig. 6. Each plotted point represents the result of a single run. Each coordinate of each point is obtained as the average of the two highest positive and two highest negative peaks (relative to the mean) of the time history. Thus emphasis is given to the highest peaks, as is appropriate for limit load determination, but the statistical base is broader than if only the single highest peak of each run had been used. For a limited number of load quantities, such as nose gear load, positive and negative peaks were substantially different, because of the proximity to strut bottoming. For these loads, only the two highest positive peaks were averaged.

For each set of twelve data points, the best-fitting straight line through the origin was then drawn. The statistically defined design level load was then obtained by entering the curve with the design value of main gear incremental load factor of 0.70. Ordinarily this entire operation was performed by computer, using a least-squares fit to the data.

Statistically defined design level values were obtained in this way for all measured airplane loads and accelerations, all gear loads, generalized accelerations in all elastic modes, and the symmetric and antisymmetric components of main gear load. Loads were obtained separately for the three airplane weight conditions giving critical loads in various parts of the airplane.

In the forward-c.g. runs, made to establish the design nose gear and forebody loads, an additional steady nose-down pitching couple was applied, such as to give an increase in the static load on the nose gear of $0.035W$ (where W is the airplane gross weight). Inclusion of this additional nose gear static load resulted in a more compressed position of the nose gear strut, hence a stiffer strut and higher incremental loads, as well as a higher static load. It was motivated by taxi load test results obtained on the P3 airplane (similar to the Electra transport) in which the steady nose gear load increased markedly with increasing

Table 3 Maximum Δn_G values in taxi

Speed, knots	Highest value of $\Delta P_V/0.5$ GW	
	With lift	No lift
30	0.31	0.29
60	0.50	0.48
90	0.38	0.50
120	0.53	0.62
Accelerating	0.53	0.70

speed, indicating a nose-down aerodynamic pitching couple. It was also felt that possibly some provision should be made for the effect of braking in combination with taxiing loads. Actually, both wind-tunnel model tests and later airplane taxi loads tests showed that for the L-1011 the nose gear load lightens with increasing speed, instead of increasing, and it is now considered that the full 0.035W increment was not necessary.

Matching Condition Generation

With the statistically defined airplane loads established, as illustrated by Fig. 6, it was still necessary to establish design conditions for stress analysis. Consequently, matching conditions were then generated, in the same general way as described earlier for gust loads.

One difference between the taxi and gust matching condition generation lay in the procedure used to phase the wing bending and torsion moments at each station. Instead of utilizing an equal-probability ellipse, defined by a calculated value of a correlation coefficient, a similar result was achieved in the taxi loads generation by employing the concept of a fictitious structural element. This concept is developed in detail in Ref. 2, but may be briefly described by reference to Fig. 7. At each wing station where bending and torsion time histories were obtained, time histories—and statistically defined design level values—were also obtained of two fictitious stresses, $q_1 = a_1B + a_2T$ and $q_2 = a_1B - a_2T$, where B is the bending moment and T the torsion moment. The coefficients a_1 and a_2 were chosen so that, in the sketch, the dash line BC would have a desired slope—i.e., one such that points B and C would represent equal percentage reductions from the design-level torsion and bending moments respectively (Point A). The alternate signs for the second term provide both of the pairs of parallel dash lines shown in the figure.

The sketch illustrates that combining design-level torsion with design-level bending (Point A) is unduly severe, as this would result in a stress in the fictitious element greater than given by the analysis. No more than the Point B torsion need be combined with the design-level bending, and no more than Point C bending need be combined with design-level torsion. Actually, even Points B and C are slightly more severe than required, as additional fictitious structural elements could be defined that would round off the corners at B and C just as the dash line cuts off the corner at A.

The concept of a fictitious structural element is an outgrowth of a procedure formerly used[2] to define phasings in power-spectral gust loads work, prior to the use of correlation coefficients and equal-probability ellipses. Wing front and rear beam shear flows were obtained from the power-spectral analysis and used as a guide in phasing the shear and torsion, in the same way that points B and C were established in Fig. 7. It became evident, however, that the phasing of the shear and torsion must depend only on the over-all dynamic characteristics of the airplane—weights, SIC's, etc.—and not at all on its structural arrangement. Consequently, if a computed stress were to be used as a key to the phase characteristics, this stress could as well be that in a fictitious element as a real one. It is believed that the fictitious element concept will remain useful in gust as well as taxi loads work—for example, in a mission analysis gust loads determination in which no single segment predominates and the values of ρ (or, equally, the characteristics of the 1-g loading) vary substantially from segment to segment.

Generally the generation of taxi matching conditions proceeded much faster than the generation of gust matching conditions, probably because of the absence of aerodynamic loadings. Elementary distributions consisted of unit symmetric main gear load reacted by pitch and plunge inertia, unit antisymmetric main gear load reacted by roll inertia, unit nose gear load reacted by pitch and plunge inertia, and inertia forces associated with unit generalized acceleration in each of the elastic modes used in the time history analysis.

References

[1]Stauffer, W. A., Lewolt, J. G., and Hoblit, F. M., "Application of Advanced Methods to Design Loads Determination for the Lockheed L-1011 Transport," *Journal of Aircraft,* Vol. 10, No. 8, Aug. 1973, pp. 449–458.

[2]Hoblit, F. M., Paul, N., Shelton, J. D., and Ashford, F. E., "Development of a Power-Spectral Gust Design Procedure for Civil Aircraft," FAA-ADS-53, Jan. 1966, Federal Aviation Agency, Washington, D.C.

[3]Neuls, G. S., Maier, H. G., Leverick, T. R., Robb, E. A., and Webster, I. J., "Optimum Fatigue Spectra" (second phase report), ASD TR61-235, April 1962, U.S. Air Force, Wright-Patterson Air Force Base, Ohio.

[4]Watkins, C. E., Woolston, D. S., and Cunningham, H. J., "A Systematic Kernel Function Procedure for Determining Aerodynamic Forces on Oscillating or Steady Finite Wings at Subsonic Speeds," TR R-48, 1959, NASA.

[5]Fuller, J. R., Richmond, L. D., Larkins, D. C., and Russell, S. W., "Contributions to the Development of a Power-Spectral Gust Design Procedure for Civil Aircraft," FAA-ADS-54, Jan. 1966, Federal Aviation Agency, Washington, D.C.

[6]Batterson, S. A., "Recent Data on Tire Friction During Landing," RM L57D19b, June 1957, NASA.

[7]Batterson, S. A., "Investigation of the Maximum Spin-Up Coefficients of Friction Obtained During Tests of a Landing Gear Having a Static-Load Rating of 20,000 Pounds," MEMO 12-20-58b, Dec. 1958, NASA.

[8]Hall, A. W. and Kopelson, S., "The Location and Simulated Repair of Rough Areas of a Given Runway by an Analytical Method," TN D-1486, Oct. 1962, NASA.